Article

Carboxymethylated Dextran-Modified N-Heterocyclic Carbene Self-Assembled Monolayers on Gold for Use in Surface Plasmon Resonance Biosensing

Zhijun Li, Kim A. Munro, Mina Narouz, Bin Hao, Cathleen M. Crudden, J Hugh Horton, and Hongxia Hao

ACS Appl. Mater. Interfaces, **Just Accepted Manuscript** • DOI: 10.1021/acsami.7b13114 • Publication Date (Web): 19 Oct 2017

Carboxymethylated Dextran-Modified N-Heterocyclic Carbene Self-Assembled Monolayers on Gold for Use in Surface Plasmon Resonance Biosensing

Zhijun Li,[†,‡] *Kim Munro,*[§] *Mina R. Narouz,*[‡] *Bin Hao,*[†] *Cathleen M. Crudden,*[‡,¶] *J. Hugh Horton,*[‡]* *Hongxia Hao*[†]*

[†] Collaborative Innovation Center of Judicial Civilization and Key Laboratory of Evidence Science, China University of Political Science and Law, Beijing, 100088, China

[‡] Department of Chemistry, Queen's University, Kingston, Ontario, K7L 3N6, Canada

[§] Protein Function Discovery Facility, Queen's University, Kingston, Ontario, K7L 3N6, Canada

[¶] Institute for Transformative Bio-Molecules (ITbM-WPI), Nagoya University, Chikusa, Nagoya, 464-8602, Japan

ABSTRACT Surface chemistry is a key enabler for various biosensing applications. Surface plasmon resonance (SPR)-based biosensors routinely employ thiol-based chemistry for the linker layer between gold-coated support surfaces and functional biosensor surfaces. However, there is a growing awareness that such sensor surfaces are prone to oxidation/degradation problems in the presence of oxygen, and previous efforts to improve the stability have shown limited advancements. As an alternative, recent studies employing N-heterocyclic carbene (NHC) self-assembled monolayers (SAMs) deposited on gold have shown significant promise in this

area. Here, we describe a sensor surface employing an NHC SAM to couple a modified carboxymethylated (CM) dextran onto a gold surface. Such a dextran matrix is also used for affinity chromatography, and is the most commonly employed matrix for commercial biosensor surfaces today. The performance reliability of the dextran-modified NHC chip to act as an alternative biosensing platform is compared with that of a thiol-based commercial chip in proof-of-concept tests. The resultant NHC sensor surface shows higher thermal stability compared to thiol analogues. Moreover, the plasma protein/drug and antibody/antigen interactions were validated on the NHC-based dextran chip and showed similar performance as compared to the thiol-based commercial chip. Ultimately, this study shows the strong potential applicability of chemical modifications to gold surfaces using NHC ligands for biosensing applications.

KEYWORDS N-heterocyclic carbenes, thiols, surface plasmon resonance-based biosensing, carboxymethylated dextran, non-specific protein adsorption, stability

1. INTRODUCTION

Self-assembled monolayers (SAMs) are an important class of nanomaterials in terms of their potential in many fields, including electronic device fabrication, biosensing, and surface protection.[1,2] Among different types of SAMs, thiols deposited by adsorption from organic solvents onto gold surfaces to form ordered monolayers have emerged as one of the most widely studied and practical forms of nanotechnology.[1] Arguably the most successful application of thiol-based SAMs has been to surface plasmon resonance (SPR)-based biosensors.[3] SPR exploits the evanescent wave phenomenon to enable real-time monitoring of biomolecular interactions occurring between ligands that are attached to the surface of a biosensor device and analytes in solution.[3] For successful SPR experimentation, the sensor surface must provide a stable base for

ligand attachment which allows the ligand to be both accessible and specific to the analyte, and which is capable of withstanding a wide range of chemical conditions, both during the detection and the regeneration stages of the biosensing experiment.[4]

Extensive efforts have been dedicated to the development of versatile biosensor surfaces employing thiol-based chemistry to accommodate different biomolecules.[2,5−10] However, degradation of thiol-based SAM surfaces is one of the most serious limitations for varied practical uses, even under ambient atmosphere.[11−14] Thiol SAMs containing ethylene glycol subunits are commonly used as linker layers as they show excellent resistance to non-specific protein adsorption.[13] However, the sulfur headgroups and ethylene glycol subunits are susceptible to thermal/oxidative degradation, resulting in a short shelf life.[12,13] For example, Langer *et al.* reported the loss of integrity of undecanethiol and tri(ethylene glycol)-terminated undecanethiol SAMs in biological media after 35 days.[14] The high cost and high propensity to degradation of the thiol-based commercial sensor surfaces are key obstacles for their broad deployment. Recently, organoselenium compounds have been proposed as alternatives to thiolates for SAMs on different metal surfaces; however, they still suffer from limited improvement in stability in various conditions.[15,16] Therefore, development of robust alternatives should be an important characteristic for the next generation of SAM technologies.

N-heterocyclic carbenes (NHCs) possess notable stability and have therefore emerged as promising carbon-based ligands for attachment to transition metals in numerous commercially-important applications.[17−21] We have previously demonstrated ordered NHC SAMs prepared by imidazolium salts as an alternative to thiols for attachment on gold surfaces, exploiting the enhanced affinity of the gold-carbon bond to result in notable stabilities when exposed to a variety of harsh environments.[18,21] Of note is that the N-substituted imidazole ring is commonly

present in natural products and biomolecules in human metabolism, suggesting the potential applicability of employing imidazolium in certain bio-systems.[22,23] For example, imidazolium-based lipid analogues have been developed and demonstrated potential cellular effects via membrane interactions.[23,24] Although thiol-gold linkage was still being used as part of the imidazolium ionic liquid biosensor, the utilization of imidazolium-based ionic liquid surface has also shown promise in biosensing.[25] Recently, bio-compatible NHC-protected gold nanoparticles have been developed and have also demonstrated potential application in bio-imaging.[26]

We have recently demonstrated an application of NHC-based SAMs for use as a hydrophobic association-based biosensor for the capture of lipid vesicles and the subsequent capture and detection of lipid-binding analytes.[21] We compared their biosensing properties, as well as their chemical and thermal stability, to thiol-based commercial analogues. The NHC SAM was observed to show both performance and stability behavior superior to thiol-based biosensor surfaces. Here, we explore the feasibility of employing NHC-based SAMs as linkers to support dextran-modified surfaces, arguably the most widely employed class of SPR-based biosensors. Dextran has been shown to be an ideally-suited component of biosensor surfaces, due to its stability and ability to be derivatized with a range of functional groups that facilitate coupling of biomolecules of interest.[27,28] We present a detailed characterization and validation by comparing NHC-based carboxymethylated dextran (NHC-CM) biosensor chips to commercially available thiol-based carboxymethylated dextran chips as well as a thiol-based chip synthesized by us, which we will denote here as S-CM. The commercial CM5 chip (GE Healthcare) is a general-purpose chip prepared by employing a 500 kDa dextran linked to a thiol SAM on a gold surface for biomolecular interaction analysis; the CM3 chip exhibits the same surface functionality but

employs a shorter (approximately 150 kDa) dextran matrix.[3,4] We address two main objectives: (i) exploring the thermal stability by characterizing the sensor surfaces using X-ray photoelectron spectroscopy (XPS), atomic force microscopy (AFM), contact angle (CA), and SPR-based tests for resistance to non-specific protein adsorption, and (ii) performance as a biodetector by using a plasma protein-drug interaction and an antibody-antigen interaction as model systems. This study of the NHC-supported CM dextran surface serves to illustrate the potential of NHC SAMs for further development in biosensing.

2. EXPERIMENTAL SECTION

2.1 Materials

Sodium phosphate monobasic monohydrate, sodium phosphate dibasic, sodium chloride, ferulic acid, indomethacin, naproxen, and furosemide were purchased from CNW Technologies. Disodium ethylenediamine tetraacetate, hydrogen peroxide (30 %), and methanol were obtained from Fisher. Potassium chloride was purchased from Sangon Biotech. Ammonia hydroxide (30 %) was purchased from J. T. Baker Chemical. Bromoacetic acid was obtained from Fluka. Epichlorohydrin was obtained from Aldrich. Dry methanol was purchased from EMD and polyethersulfone syringe filters were purchased from Sterlitech. Bovine serum albumin (BSA) was obtained from Shanghai Yeasen Biotech. Lysozyme, ovalbumin, human serum album (recombinant, expressed in *Pichia pastoris*), concanavalin A, fibrinogen, monoclonal anti-BSA, sodium dodecyl sulfate (SDS), 11-Mercapto-1-undecanol, dextran 6 kDa and 500 kDa (from leuconostoc) were purchased from Sigma-Aldrich. Streptavidin was obtained from Promega, and biotin anti-mouse IgG2b antibody was purchased from BioLegend. CM5 chip, CM3 chip, glycine/HCl (pH 1.5), glycine/HCl (pH 2.0), glycine/HCl (pH 2.5), glycine/HCl (pH 3.0), 50 mM NaOH, BIAtest solution, HBS-EP buffer, amine coupling Kit (N-Hydroxysuccinimide,

1-Ethyl-3-(3-dimethylaminopropyl) carbodiimide hydrochloride, ethanolamine hydrochloride-NaOH pH 8.5), and SIA kit Au (10 pieces of gold surfaces, sensor chip assembly unit, protective sheath, double-sided adhesive) were purchased from GE Healthcare. All solutions used for SPR tests were filtered through 0.22 μm filters and degassed before use, and the SPR tests were carried out at 25 ºC.

2.2 Preparation of Dextran-Modified NHC and Thiol Surfaces

The detailed preparation procedure for 5-((11-hydroxyundecyl)oxy)-1,3-diisopropyl-1H-benzo[d]imidazol-3-ium hydrogen carbonate was described in Ref 18 and 21. The overall synthetic approaches for preparing dextran-modified NHC and thiol surfaces are based on the methods of Löfås *et al.*[8] and Granqvist *et al.*[10]. The gold surfaces (SIA kit Au, GE Healthcare) were first cleaned by immersion in a mixture of NH_4OH: H_2O_2: H_2O (1:1:5) at 80 °C for 10 min, rinsed with Milli-Q water, and dried under a stream of nitrogen. Additional plasma cleaning was carried out for 10 min using a Harrick Plasma Cleaner/Sterilizer (PDG-32G). The gold surfaces were then immersed in a solution of 10 mM 5-((11-hydroxyundecyl)oxy)-1,3-diisopropyl-1H-benzo[d]imidazol-3-ium hydrogen carbonate in dry methanol for 24 h to prepare the NHC-CM surfaces;[21] similarly, the thiol-based S-CM surfaces were prepared by immersing the gold in a 5 mM 11-Mercapto-1-undecanol in ethanol: water (8:2) solution for 24 h. Subsequently, these surfaces were rinsed thoroughly with methanol and Milli-Q water, then reacted with epichlorohydrin (2% v/v) in 0.1 M NaOH for 3 h, rinsed with Milli-Q water, and transferred to a 300 g/L dextran solution (dextran strands of two different length were used: 6 kDa dextran or 500 kDa dextran) in 0.1 M NaOH for 24 h. The resultant surfaces were washed with Milli-Q water and immersed in 1.0 M bromoacetic acid in 2 M NaOH for 24 h. Finally, they were washed thoroughly with Milli-Q water, dried with an argon stream, and mounted onto a support

(SIA kit Au, GE Healthcare). To test the uniformity of individual flow cells of the NHC-based sensor surface, a view dips test[29] was performed and compared to the corresponding performance of commercial CM5 and CM3 chips. To test the homogeneity and performance of the NHC-based sensor surface, a system check test[30] (a program in Biacore 3000 control software) was carried out using a standard sucrose solution and compared to the commercial CM5 and CM3 chips.

2.3 Thermal Stability of Commercial CM3 Chip and Non-Commercial 6 kDa S CM and 6 kDa NHC-CM Chips

Both prior to and following thermal exposure treatment at 65 ºC for 24 h in air, the CM3 chip, 6 kDa S-CM chip, and 6 kDa NHC-CM chip were evaluated by XPS, AFM, CA, and non-specific protein adsorption tests. For the non-specific protein adsorption test, the proteins used consisted of lysozyme (14 kDa, *p*I = 11.35), ovalbumin (45 kDa, *p*I = 4.5), bovine serum albumin (BSA, 66 kDa, *p*I = 5.3), human serum albumin (66 kDa, *p*I = 5.3), streptavidin (66 kDa, *p*I = 6.0), concanavalin A (102 kDa, *p*I = 4.5~5.5), and fibrinogen (340 kDa, *p*I = 5.5). Each protein was dissolved in PBS buffer (10 mM phosphate, 138 mM NaCl, 2.7 mM KCl, pH 7.4) at a concentration of 0.1 mg/ml. Tests of the non-specific binding for each sensor surface were carried out using a Biacore 3000 instrument (GE Healthcare). The protocol for measuring the non-specific protein adsorption is as follows: Following initial baseline equilibration, PBS buffer was flowed over the sensor surface for 2 min, followed by injection of a protein solution for 3 min, and finally by a 5-min buffer rinse. The flow rate was maintained at 10 μl/min throughout these tests. The regenerations of the sensor surfaces were effected as follows: one 1-min injection of 50 mM NaOH for ovalbumin adsorbed surfaces, one 1-min injection of 0.5 % (w/v) SDS followed by two 1-min injections of 50 mM NaOH for fibrinogen adsorbed surfaces, and

two 1-min injections of 50 mM NaOH for lysozyme, BSA, and concanavalin A adsorbed surfaces.

2.4 Plasma Protein-Drug Interaction Performance Comparison Test

2.4.1 Immobilization of Human Serum Album

Commercial CM3 and 500 kDa NHC-CM chips prepared in our lab were used for this study. Human serum albumin (HSA) was immobilized on each sensor chip using amine coupling chemistry in PBS buffer (10 mM phosphate, 138 mM NaCl, 2.7 mM KCl, pH 7.4). The active surface was prepared by two 7-min injections of a 1:1 (v/v) mixture of 0.2 M 1-ethyl-3-(3-dimethylaminopropyl) carbodiimide hydrochloride (EDC) and 0.05 M N-Hydroxysuccinimide (NHS) at 20 μl/min. This was followed by two 10-min injections of 100 μg/ml HSA in 10 mM sodium acetate (pH 5.2). The surface was then blocked with a 10-min injection of 1 M ethanolamine (pH 8.5). An unmodified dextran surface on each chip was used as a reference surface.[31] Three 30-s injections of 50 mM NaOH were used to wash off noncovalently bound HSA to stabilize the surface. Final immobilization levels of HSA on the commercial CM3 and 500 kDa NHC-CM chips were approximately 5000 response units (RU) and 4200 RU, respectively.

2.4.2 Plasma Protein-Drug Interactions

A series of small drug molecules including indomethacin ($C_{19}H_{16}ClNO_4$, M.W. 358 Da), furosemide ($C_{12}H_{11}ClN_2O_5S$, M.W. 331 Da), ferulic acid ($C_{10}H_{10}O_4$, M.W. 194 Da), and naproxen ($C_{14}H_{14}O_3$, M.W. 230 Da) were tested as analytes for the HSA-immobilized surfaces. Drug binding studies were performed in PBS buffer (10 mM phosphate, 138 mM NaCl, 2.7 mM KCl, pH 7.4) containing 1 % DMSO. Analyte concentrations tested were as follows: Indomethacin (7.5 ~ 125 μM), furosemide (3.2 ~ 200 μM), ferulic acid (6.3 ~ 200 μM), and

naproxen (6.3 ~ 200 μM) in 2-fold dilution series. Triplicate injections of each drug concentration were performed over the reference and HSA surfaces at a flow rate of 30 μl/min. Each cycle consisted of a 1-min waiting period for monitoring of the baseline stability, then the drug/HSA complex was allowed to associate and dissociate for 60 s and 30 s, respectively, followed by a 30-s buffer injection to prevent carryover between analyte injections. No regeneration was required as each compound dissociated from the HSA surface within minutes.[4,31] The reference surface was used as a control for drugs binding to the dextran surface.[31] Reference-subtracted data was processed following subtraction of buffer injection sensorgrams (double referencing method).[31,32] Steady-state affinity (response at equilibrium plotted against sample concentration) was used to analysis the interactions between drugs and HSA.[31,33,34]

2.5 Antibody-Antigen Interactions Performance Comparison Tests

2.5.1 Immobilization of BSA

PBS buffer (10 mM phosphate, 138 mM NaCl, 2.7 mM KCl, pH 7.4) was used as the running buffer and BSA was immobilized onto the NHC-CM chips using amine coupling chemistry. The active surfaces of the 500 kDa NHC-CM and 6 kDa NHC-CM chips were prepared by activation of two consecutive 7-min injections of a 1:1 mixture of 0.2 M EDC/0.05 M NHS at a flow rate of 20 μl/min. Two 10-min injections of 100 μg/ml BSA in 10 mM sodium acetate (pH 4.2) were immobilized on these surfaces. Subsequently, the resultant surfaces were blocked with a 10-min injection of 1 M ethanolamine (pH 8.5). Final immobilization levels of the BSA on the 500 kDa NHC-CM and 6 kDa NHC-CM chips were approximately 3800 RU and 1980 RU, respectively. An unmodified surface was used as reference surface for each chip.

2.5.2 Antibody-Antigen Interactions (Anti-BSA/BSA)

Anti-BSA was diluted with the running buffer to produce a series of final concentrations of 5.5, 11, 22, 44, 88, 175, 350 nM for tests on the 500 kDa NHC-CM chip, and 11, 88, 350 nM for the 6 kDa NHC-CM chip, respectively. For both 500 kDa NHC-CM and 6 kDa NHC-CM BSA-immobilized surfaces, kinetic interaction tests were performed at a flow rate of 40 µl/min. For each anti-BSA concertation, association/dissociation behavior was tested by triplicate injections, each having equal 6-minute association and dissociation phases. In addition, corresponding buffer injections were performed on both surfaces. Between anti-BSA injections, surface regeneration was performed by two 30-second injections of 50 mM NaOH followed by a 2-min buffer equilibration. 50 mM biotin anti-mouse IgG2b antibody was used as a negative binding control on the 500 kDa NHC-CM and 6 kDa NHC-CM chips. Reference-subtracted data was fitted using the 1:1 Langmuir binding model following double-reference subtraction of buffer injection profiles.[32]

2.6 Surface Characterization

X-ray photoelectron spectroscopy (XPS) was performed on a Thermo Instruments 310-F Microlab (Thermo Fisher, UK) to evaluate the surface composition of samples. Spectra were obtained with a monochromatic Mg *Kα* X-ray source (1253.6 eV) at 15 kV anode potential with 20 mA emission current. Thermo Scientific Avantage software (Thermo Fisher, UK) was used for data processing. Spectra obtained were normalized to the Au $4f_{7/2}$ at 84.0 eV, and were fitted with Gaussian-Lorentzian (70%: 30%) peaks after subtraction of a Shirley background. Contact angle measurements (CA) were carried out on a DataPhysics OCA 15Pro optical instrument (DataPhysics Instruments GmbH, Germany) at ambient temperature by placing 2 µl of Milli-Q water onto the sensor surface. The average CA values were obtained by measuring four different positions on each sample surface. Surface morphologies and roughness of samples were obtained

using atomic force microscopy (AFM) in a tapping mode on a Veeco multimode instrument (Veeco Instruments Inc., USA) equipped with a Nanoscope IIIa controller.

3. RESULTS AND DISCUSSION

3.1 Synthesis and Surface Characterization of the NHC-linked CM SPR Sensors

Here, three types of sensor surfaces were used, as shown schematically in Figure 1: (a) the commercial carboxymethylated dextran chips (CM3 or CM5) which have the same surface functionality but with different length of dextran strands, (b) a thiol-based 6 kDa carboxymethylated dextran strand version prepared by us (S-CM) and (c) the NHC-linked (6 kDa or 500 kDa NHC-CM dextran strands) carboxymethylated surfaces. For the commercial CM series chips, 16-mercaptohexadecan-1-ol was used as a chemical linker to attach a dextran layer.[8] The thiol linker used to prepare the S-CM chip was mercaptoundecanol, which is the same as previously used by Granqvist *et al.*.[10] For the NHC-CM surface, (5-((11-hydroxyundecyl)oxy)-1,3-diisopropyl-1H-benzo[d]imidazol-3-ium hydrogen carbonate) was used as the NHC linker. The surface characterization of this hydroxyl-NHC self-assembled monolayer (SAM) on gold was studied by X-ray photoelectron spectroscopy (XPS) and contact angle (CA) measurements, as shown in supporting information Figure S1.

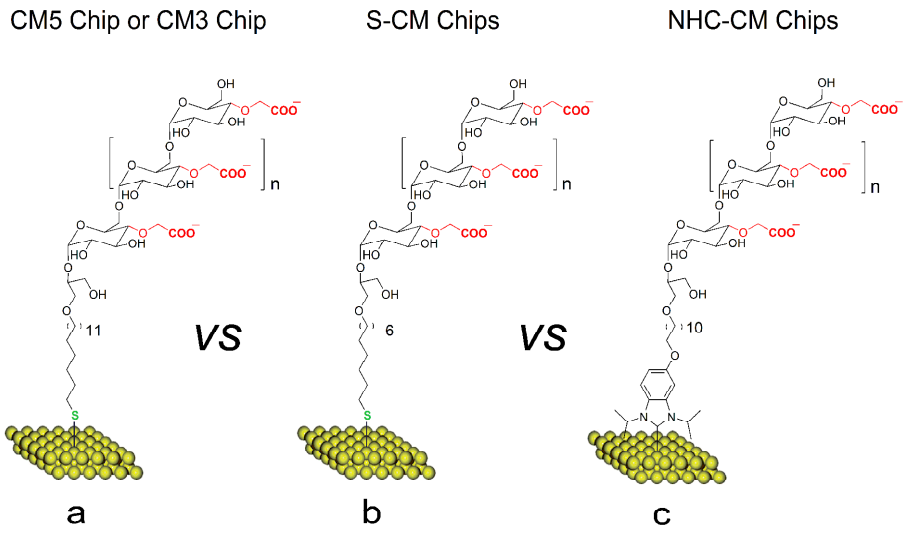

Figure 1. Schematic illustration of (a) the commercially available CM5 (n = 3122) or CM3 (n = 937) chips, (b) the thiol-based S-CM version prepared by us and (c) NHC-based sensor chips (6 kDa, n = 37; 500 kDa, n = 3122).

Figure 2 illustrates the preparation procedure for the dextran-modified NHC surface. Hydroxyl-terminated NHC molecules were first self-assembled on the gold surface as a chemical linker for subsequent attachment of a dextran layer. Activation of the hydroxyl groups was carried out using basic epichlorohydrin to form epoxides. Dextran (either 6 kDa or 500 kDa) in basic solution was used to covalently bind to the NHC-epoxides. Then the dextran-coated surface was treated with bromoacetic acid, resulting in a CM dextran layer linked to the NHC surface.[8] Note that Figure 2 shows an ideal case: the dextran might not bind from the chain end to the epichlorohydrin, but instead from a random unit in the chain. This surface is negatively charged in neutral buffer with the dextran chains repelling each other, giving rise to an expansion of the hydrogel with high binding capacity and accessibility for biomolecules.[3] As described later, further chemical steps can then be used to immobilize a wide range of biomolecules to the

carboxyl groups of the dextran on the sensor surface.[3–5] A similar approach was applied to the synthesis of thiol-based (6 kDa) S-CM chip (Figure S2).

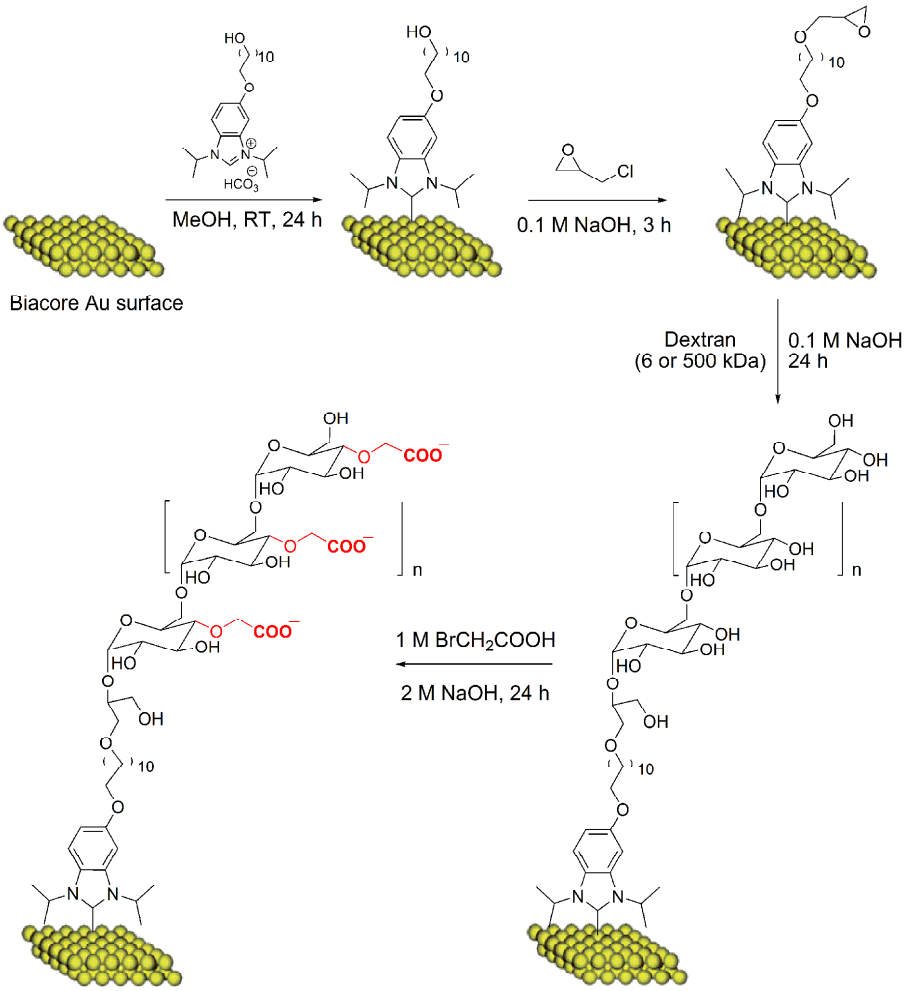

Figure 2. Schematic illustration of the preparation of carboxymethylated dextran-modified NHC sensor surface.

XPS was performed to determine the changes in surface composition of the various 6 kDa carboxymethylated dextran surfaces before and after exposure to 65 ºC in air for 24 h (Figure 3).

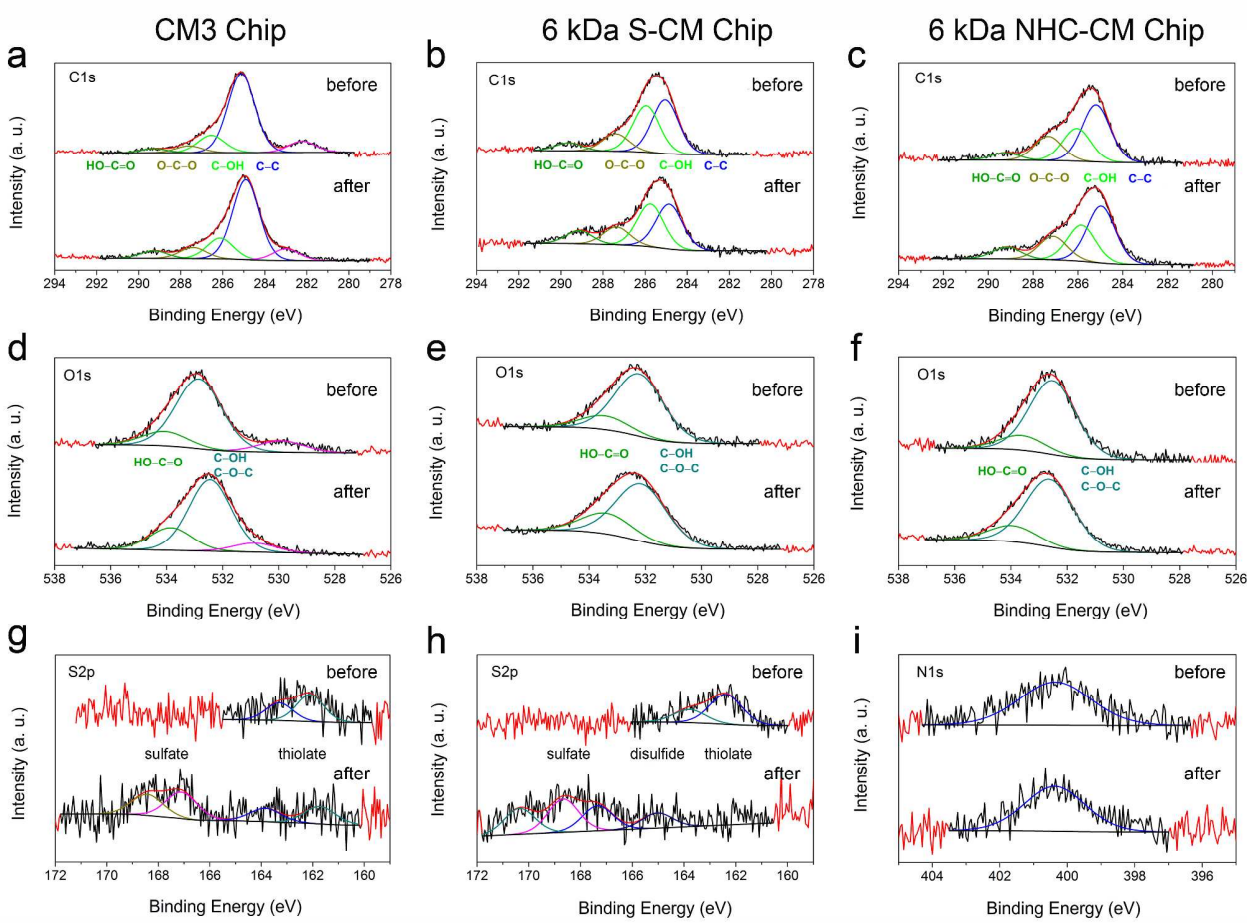

Figure 3. XPS of the commercial CM3 (a, d, g), 6 kDa S-CM (b, e, h) and NHC-CM (c, f, i) SPR sensor chips before and after thermal exposure at 65 ºC in air for 24 h. For the C 1s spectra, the magenta, blue, green, dark yellow, and olive lines correspond to contributions arising from metal carbide, C–C / C–H, C–OH, O–C–O, and HO–C=O species, respectively. For the O 1s spectra, the magenta, dark cyan, and olive lines represent metal oxide, C–OH / O–C–O, and HO–C=O, respectively.

The C 1s spectrum for the three chips tested (Figures 3a,b,c and Table S1) shows contributions from five components: HO–C=O (observed at 289.5 ± 0.2 eV), O–C–O (287.5 ± 0.1 eV), C–OH (286.1 ± 0.2 eV), C–C / C–H (285.1 ± 0.1 eV),[35–37] and (for the CM3 chip only) metal carbide at 282.2 eV. Assuming every linker molecule is terminated with a dextran strand, there are some

tens to hundreds of dextran units per linker unit present. Therefore, the C and O spectra will be dominated by the dextran species. Furthermore, the relative distribution of intensities between the four types of carbon species should indicate the relative density of carboxylate molecules within the dextran matrix. A reliable quantitative determination of the relative peak intensities is difficult, due to the relatively low inherent resolution of the XPS spectrometer. However, some general observations can be made. While all three sensor surfaces showed a relative increase in intensity of the HO–C=O peak, indicating degradation of the partial thermal degradation of the dextran strands, the effect was markedly less pronounced in the case of the commercial CM3 chip and greatest for the S-CM chip.

The O 1s spectra for the three chips tested (Figures 3d,e,f) shows contributions for three oxygen bonding components: HO–C=O (533.8 ± 0.3 eV), C–OH / O–C–O (532.6 ± 0.3 eV), and metal oxide (again, in the CM3 case only) at 529.9 eV. Similar to the observations for the C 1s spectra, a comparison of the O 1s for the three surfaces before and after thermal exposure shows a relative increase in the intensity of the HO–C=O peak compared to the C–OH / O–C–O peak in each case, consistent with some degree of degradation of the dextran matrix. The unexpected metal carbide and oxide peaks which we observed in both the C 1s and O 1s spectra of the CM3 chip exclusively may have been an artifact from adhesive residue remaining after removal of the CM3 chip from its plastic mount; however, we did not investigate this issue further in this study.

We may also determine the relative C1s:O1s area ratios (Table S2). These decrease in each case, indicating some degree of oxidation of the dextran matrix. The effect is most significant for the S-CM chip, with a 49 % decrease, somewhat less pronounced for the NHC-CM chip at 34 %, and least for the commercial CM3 chip at 25 %. Thermal degradation of dextran might

result from the free radical oxidation of carbon 6 of glucopyranosyl units with the formation of carboxyl groups and water.[38]

While the dextran layer on the CM3 chip appears more stable than either of the chips produced in our lab (Table S2), the XPS from the linker layer itself shows evidence of quite different behavior (Table S3). For both thiol-based sensor surfaces (CM3 and S-CM), the S 2p spectrum (Figures 3g,h) shows the presence of a doublet S $2p_{3/2,1/2}$ spectrum.[39] The S 2p peak at 162.2 ± 0.1 eV observed for both CM3 and S-CM sensor chips before thermal exposure is consistent with sulfur headgroups bound to a gold surface as a thiolate species.[39–41] Following thermal exposure, the thiolate peak intensity is almost completely suppressed, while a new S 2p peak consistent with the presence of a sulfate appeared at 167.2 ± 0.1 eV.[39–41] In addition to this change, the S 2p spectrum for the S-CM sensor chip also showed some evidence of a disulfide species at 165.0 eV.[14] These changes are consistent with oxidation of the thiol linker on the gold surface following thermal exposure. By contrast, on the NHC-CM chip, the N 1s spectrum (Figure 3i) consists of a single peak at 400.4 eV,[42,43] which is unchanged following thermal exposure, confirming a high stability of the linker component against degradation/oxidation as compared to thiol-supported surfaces.

Atomic force microscopy (AFM) images for the CM3, 6 kDa S-CM, and 6 kDa NHC-CM chips are shown in Figure S3. A similar globular morphology has been previously observed for dextran coated surfaces.[44,45] Both the S-CM and NHC-CM exhibited a greater surface roughness (Table S4), and larger average particle size than the CM3 chip. They also showed more significant increases in surface roughness following thermal exposure (Table S4). This seems consistent with greater degradation of the dextran layer taking place in these chips.

Finally, we also carried out contact angle measurements of the sensor surfaces before and after thermal exposure. The results are summarized in Table S5. Both thiol-based chips exhibited a contact angle of 53°, whereas the NHC chip was more hydrophobic, with a contact angle of 68°. The contact angle of all three samples increased following thermal exposure to an average value of 85°, consistent with our observations using XPS that indicated degradation of the dextran layer. The higher contact angle exhibited by the NHC chip is consistent with the lower adsorption density of NHCs on Au (3.5 molecules/nm^2) as compared to thiols (4.6 molecules/nm^2 for a typical alkanethiol)[18,21,46]. A less tightly packed NHC linker, and hence dextran overlayer, should result in an overall more hydrophobic surface. Nonetheless such a less densely packed NHC linker might be an advantage if an NHC-supported dextran surface is to be used in biosensing. High molecule-weight analytes are likely to agglomerate in the upper layer of densely a more packed thiol-supported dextran matrix, preventing further diffusion of analytes to be the lower parts of the dextran layer to bind ligand molecules.[3]

In summary, the surface analysis data show that in the case of the NHC-CM chip, thermal exposure under ambient conditions leads to little or no degradation of the linker layer; the thiol linker, however, is strongly oxidized. On the other hand, the dextran layer of the commercial CM3 chip appears to be relatively resistant to thermal degradation compared to the NHC-CM chip. Of course, our dextran deposition process has not had the benefit of a full optimization as has been undergone by the commercial CM3 product. What is clear, however, is when the NHC-CM chip is compared to the thiol-based carboxymethylated dextran S-CM chip, as produced in our hands, both the linker and dextran layer show significantly less thermal stability.

3.2 SPR Characterization of the NHC-CM Surface

The observed dip in reflectance amplitude versus angle of reflection is typically used as a diagnostic test of SPR sensor chip surface uniformity.[3,29,47] When compared between individual flow cells on a single sensor chip, they are also an indication of overall performance. Comparing the dips obtained from the 4 flow cells for the 6 kDa NHC-CM to those obtained for the commercial CM5 and CM3 sensor surfaces (Figure S4), it is observed that the 6 kDa NHC-CM surface has a slightly smaller dip minimum; however, in all cases the individual dip profiles on the 6 kDa NHC-CM surface were symmetrical and homogeneous, both with respect to each other and when compared to those on CM5 and CM3. An overall system check test[30] performed on 6 kDa NHC-CM chip was similar to that obtained on both the CM5 and CM3 chips, with all parameters within specified limits (Figure S5) as defined by the manufacturer of the SPR system. This procedure generates a report for the system, which contains testing results for Integrated μ-Fludic Cartridge (IFC), two syringe pumps, and needle, etc.[30] A uniform dextran sensor chip is important for successful use in this test to give reliable results. Together, these features indicate that the NHC SAM is capable of acting as a template for a homogeneous sensor surface which has a similar dynamic range to that observed for the commercial thiol-based chips.

Having conformed the homogeneity of the NHC-based platform to support a dextran surface, we next studied the basic operational characteristics of the CM chips. One important property of an SPR sensor is the degree of non-specific protein adsorption. High non-specific protein adsorption will lead to a large signal background, and may also block access to adsorption sites for the target analyte, reducing overall sensitivity. We therefore measured the degree of non-specific adsorption in PBS buffer, both before and after thermal exposure of the SPR sensor surfaces at 65 ^{o}C under ambient conditions. The adsorption profiles of 7 common proteins were compared on the thiol-supported CM3, 6 kDa S-CM and 6 kDa NHC-CM chips (Figure S6 and

Table 1). The proteins chosen display a range of sizes and charges, with *p*I varying from 4.5 to 11.35 and molecular weight ranging from 14 kDa to 340 kDa.

Table 1. Effect of thermal exposure on non-specific protein adsorption of commercial CM3, and non-commercial 6 kDa S-CM and 6 kDa NHC-CM chips.

	Non-specific adsorption (RU)					
Protein 0.1 mg/ml	Commercial CM3		6 kDa S-CM		6 kDa NHC-CM	
	Before[a]	After[b]	Before[a]	After[b]	Before[a]	After[b]
Lysozyme (14 kDa)	27 ± 4	948	107 ± 10	1161	74 ± 1	358
Ovalbumin (45 kDa)	2 ± 1	109	4 ± 1	196	3 ± 0.2	23
Bovine serum albumin (66 kDa)	26 ± 5	479	41 ± 8	797	20 ± 1	321
Human serum album (66 kDa)	183 ± 21	466	167 ± 6	731	239 ± 15	300
Streptavidin (66 kDa)	34 ± 2	72	19 ± 3	57	15 ± 3	20
Concanavalin A (102 kDa)	367 ± 5	1291	91 ± 4	1260	145 ± 11	704
Fibrinogen (340 kDa)	137 ± 20	2624	117 ± 12	3570	236 ± 20	2280

[a] Values given, before thermal exposure, as response units with standard deviations and relative standard deviations for n=3.

[b] Values given, after thermal exposure, as response units for n=1.

Table 1 demonstrates that, prior to thermal exposure, non-specific protein adsorption on the 6 kDa NHC-supported surface in PBS buffer was lower than on the CM3 surface for 3 of 7 proteins studied, and lower than on the 6 kDa S-CM surface for 4 of 7 proteins. For ovalbumin, bovine serum albumin, and streptavidin, the NHC-CM surface shows lower or similar non-specific protein adsorption ability compared to CM3 and S-CM surfaces, whereas for human serum album and fibrinogen, the NHC-CM surface exhibits a slightly higher non-specific protein adsorption ability relative to CM3 and S-CM surfaces. As for lysozyme and concanavalin A, the

NHC-CM surface displays either lower or higher non-specific protein adsorption ability as compared to CM3 and S-CM surfaces. Overall performance of all three chips was comparable, regardless of the protein studied. Following thermal exposure, an increase in non-specific adsorption was observed for all three sensor chips. However, this increase was significantly greater on both thiol-linked sensors, with adsorption of all 7 proteins observed to be lower for the 6 kDa NHC-CM surface than either of the thiol-supported surfaces.

Generally, as a protein approaches the dextran surface, there is a decreased degree of freedom (entropy) of the dextran layer. This trend results in the steric repulsion of the dextran strands from one another to repel adsorbed protein to make the system more thermodynamically stable.[48] In addition, electrostatic attraction/repulsion, buffer pH and *p*I of the different proteins, as well as different charge densities among commercial CM sensor surface and our self-synthesized sensor surfaces would also contribute to the non-specific protein adsorption behaviors.[45,49] At 150 kDa, the CM3 chip has one of the shorter dextran matrices available commercially,[4,47] but it is still higher compared to the 6 kDa dextran strand used in our S-CM and NHC-CM chips. All else being equal, this should result in a lower non-specific protein adsorption for the CM3 chip, as the hydrophilic dextran layer will increase in density and lead to a greater steric repulsion effect.[10,48] As the same dextran was used to prepare both our S-CM and NHC-CM chips, if the dextran density itself is the only factor, they should show comparable behavior to one another. This is indeed the case, and any slight improvement in non-specific adsorption seen in the NHC-based sensor is likely due to the lower hydrophilicity of the NHC linker itself, as well as the fact that the NHC SAM is known to have a lower overall density on the gold surface than the corresponding thiol SAM,[18,21,46] and hence a relatively lesser steric demand between the more widely spaced supported dextran molecules.

Upon heating, all three chips decrease in performance, in the sense that all three support a greater degree of non-specific protein adsorption. This is certainly consistent with the XPS and contact angle results, which showed a degradation of the dextran layer, and overall increase in surface hydrophobicity. In particular, it is notable that the most hydrophobic protein – fibrinogen – shows the greatest increase in non-specific adsorption, consistent with this interpretation. The XPS results also showed that both the thiol linked sensors – CM3 and S-CM – showed significant degradation of the linker layer itself, while the NHC remains intact. Our observation that NHC-based sensor shows the least degree of performance degradation after heating is again consistent, as in this case, only the dextran matrix itself is affected by heating, but not the underlying linker layer. Overall, the protein adsorption results show that the CM dextran-modified NHC surface exhibits effectiveness in preventing non-specific adsorption of proteins, its performance characteristics are comparable to the thiol-based version and, following thermal exposure, shows arguably superior resilience and performance compared to the thiol analogues.

3.3 Plasma Protein-Drug Interactions on Commercial CM3 and Non-Commercial 500 kDa NHC-CM Chips

In the pharmaceutical development process, one test parameter is to measure the affinity of small molecular drug targets against plasma proteins to understand their absorption, distribution, metabolism, and excretion (ADME) characteristics within the human body.[31,33] SPR-based biosensors can provide such information on plasma protein-drug interactions and have been demonstrated to be powerful tools for drug discovery.[4]

To validate the performance of the NHC-supported biosensor surfaces using drug-protein binding as a model system, a 500 kDa NHC-CM chip was used here. The larger molecular

weight dextran layer is expected to have a higher surface density of carboxymethylated dextran covalently attached to the NHC-linker, resulting in a higher binding capacity and hence greater sensitivity to low molecular weight compounds.[4] Human serum album (HSA) protein was immobilized on the chip surface for use in a series of binding tests with a selection of drugs as analytes.

A schematic of this process is shown in Figure 4a. Amine coupling provides a simple and straightforward method to covalently attach ligands to the dextran surface for use in biosensing.[3,4] The first step is the generation of reactive N-hydroxy succinimidyl (NHS) esters from carboxyl groups on the dextran by derivatization with 1-ethyl-3-(3-dimethylaminopropyl) carbodiimide hydrochloride (EDC) and NHS. The second step is the nucleophilic coupling of these active NHS esters with ε-amine groups of lysine residues or primary amino groups of biomolecules to form amide bonds. This step proceeds via electrostatic attraction forces between positively charged protein and negatively charged dextran matrix at a pH value between 4 ~ 5.5.[3,4] Therefore, a high local concentration of protein accumulates in the dextran matrix, giving rise to the formation of covalent bonds between them. Finally, the unreacted NHS esters on the surface are blocked by ethanolamine at a pH of 8.5, without affecting the remaining negatively charged carboxymethyl groups and hydroxyl groups in the dextran matrix.[3]

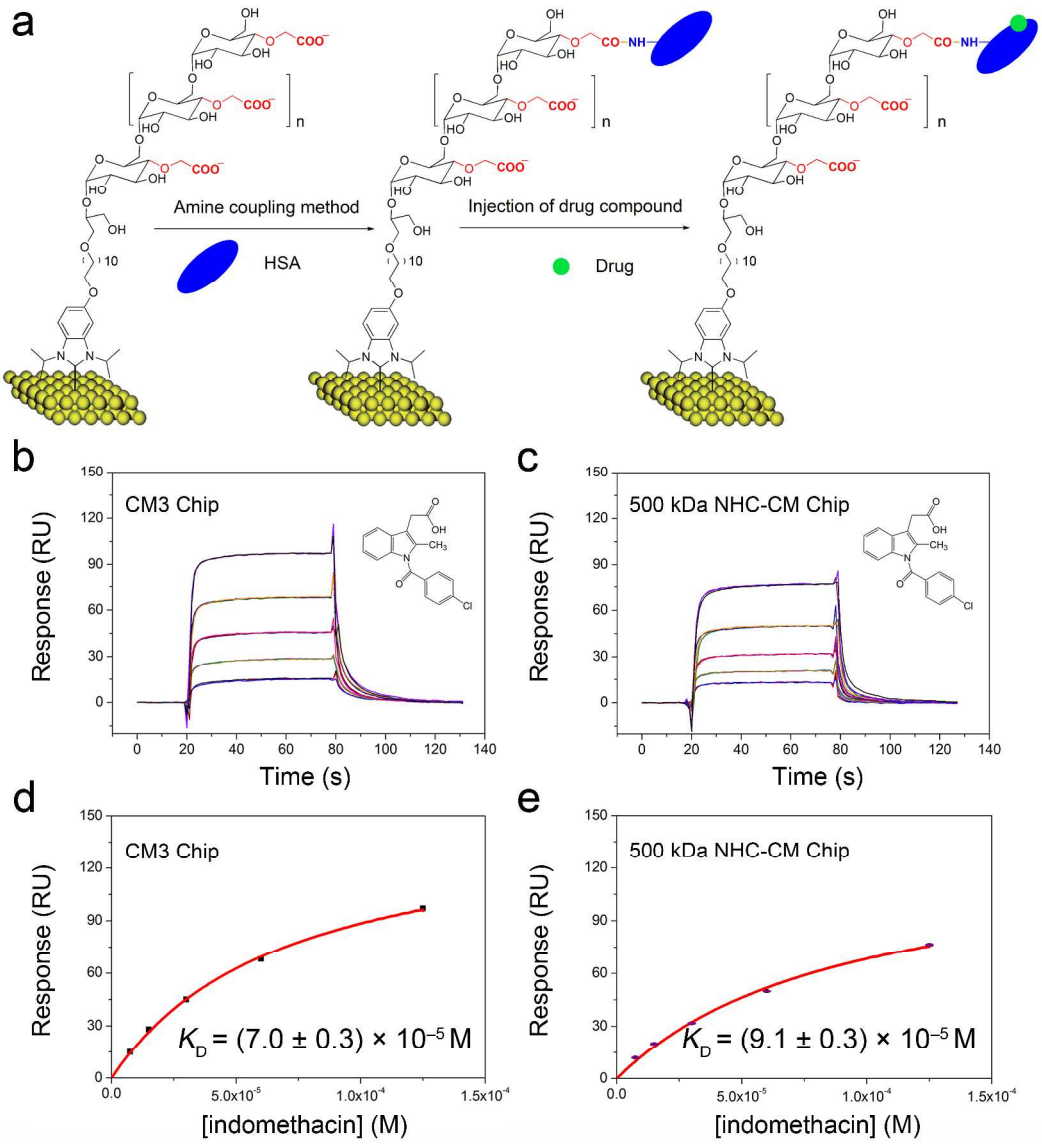

Figure 4. (a) Schematic depicting HSA immobilized on 500 kDa NHC-CM chip surface by amine coupling chemistry, followed by interaction with drug compounds. Binding sensorgrams are displayed as overlay plots from triplicate 1-min injections of indomethacin (7.5–125 μM) in 2-fold dilutions (reference-subtracted) over HSA-bound surfaces on (b) commercial CM3 and (c) 500 kDa NHC-CM chips. A steady-state model (see text) fit to determine the equilibrium dissociation constant, K_D, for indomethacin/HSA interactions on a (d) commercial CM3 and (e) 500 kDa NHC CM SPR sensor chip.

Figures 4b and c show the binding/dissociation curves for the indomethacin/HSA interaction obtained using both the commercial CM3 chip and the 500 kDa NHC-CM chip. At t = 0 s, buffer was flowed over the HSA pre-immobilized sensor surface. At t = 20 s, a solution of drug compound was passed over the pre-immobilized BSA surface, followed by the formation of drug-HSA complex on the sensor surface (association phase). Notably, an equilibrium plateau was obtained during the association phase, along with a return to the baseline during the dissociation phase (beginning at t = 80 s), exhibiting a square wave curve over the range of concentrations tested on both surfaces. These concentration-dependent and superimposable binding curves from triplicate injections on the NHC platform demonstrate that the binding assays were very reproducible (Figure 4c) and similar to the interactions on the commercial CM3 chip (Figure 4b).

The dissociation constant (K_D) for the indomethacin/HSA binding interaction may also be evaluated from an analysis[3] of the binding/dissociation curves in Figure 4. The affinity constant, K_A, of the indomethacin-HSA complex (AB) can be derived from the relationship between response at equilibrium R_{eq} and indomethacin concentration (C) by employing a steady-state affinity model.[33,34,50] A and B are the drug and HSA protein, respectively, and the net rate of complex formation is:

$$A + B \leftrightharpoons \mathrm{AB} \quad (1)$$

with association and dissociation rate constants k_a and k_d, respectively. Assuming that the concentration of indomethacin in solution, C, is effectively constant under the adsorption conditions used here, the equilibrium binding capacity, R_{eq}, may be determined to be

$$R_{eq} = \frac{CR_{max}}{K_D + nC} \quad (2)$$

where R_{max} is the maximum binding capacity of the surface to indomethacin; $K_D = k_d/k_a$ the dissociation constant; and n is a steric interference factor that used to compensate for steric blocking of additional binding sites by a single analyte molecule (default value 1).[50] The R_{max} obtained from the BIAevaluation software for the commercial chip and 500 kDa NHC-CM chip were 148 RU and 131 RU, respectively.

Figures 4.4d and e show the steady-state fitting of the indomethacin/HSA interactions using Equation 2 for both sensor surfaces. The equilibrium dissociation constant (K_D) of indomethacin/HSA interaction for the commercial chip was determined as $(7.0 \pm 0.3) \times 10^{-5}$ M, while for the 500 kDa NHC-CM chip was $(9.1 \pm 0.3) \times 10^{-5}$ M. Both data agree well with the literature value of 2.25×10^{-5} M.[51]

A series of binding tests/kinetic analysis of HSA with the small drug molecules furosemide, ferulic acid, and naproxen were also carried out to further validate the performance of the NHC-based platform (Figures S7 to S9). In each case (Figure 4 and Figures S7 to S9), the responses from these triplicate injections (in each concentration) are identical, indicating that the binding assays were stable throughout the course of the experiments performed on both the thiol- and NHC-based platforms.[4,32] Comparing these results, the character of the binding curves, as well as the associated steady-state binding levels and derived binding constants demonstrates that 500 kDa NHC-CM chip can perform similarly to the commercial CM3 chip. Moreover, these data are also very similar to previous literature values (Table S6), even though different experimental conditions were used in previous reports. These results validate the potential use of the NHC-based platform in biosensor technology to collect reliable kinetic data on small molecules binding to macromolecular targets.

3.4 Antibody-Antigen Interactions on 500 kDa NHC-CM and 6 kDa NHC-CM Chips

Surface functionalization by chemically attaching a bioreceptor to obtain a reproducible surface that enables the sensitive and specific recognition of analyte is important in biology, immunology, and pharmacology.[52–54] Thus, to further validate the performance of the NHC sensor surfaces, monoclonal anti-BSA and BSA were used as a model system for high-affinity antibody-antigen interactions, as the SPR chip performance can be readily compared to that published in earlier studies.[55–57] To study this interaction, BSA was first immobilized onto the dextran-modified NHC surfaces (500 kDa NHC-CM and 6 kDa NHC-CM) using amine coupling chemistry, then monoclonal anti-BSA was injected over the reference and BSA surfaces (Figure 5a). Then we monitored the real-time binding kinetics of the antibody to antigen on the sensor surfaces, and compared our experimental results to literature values.

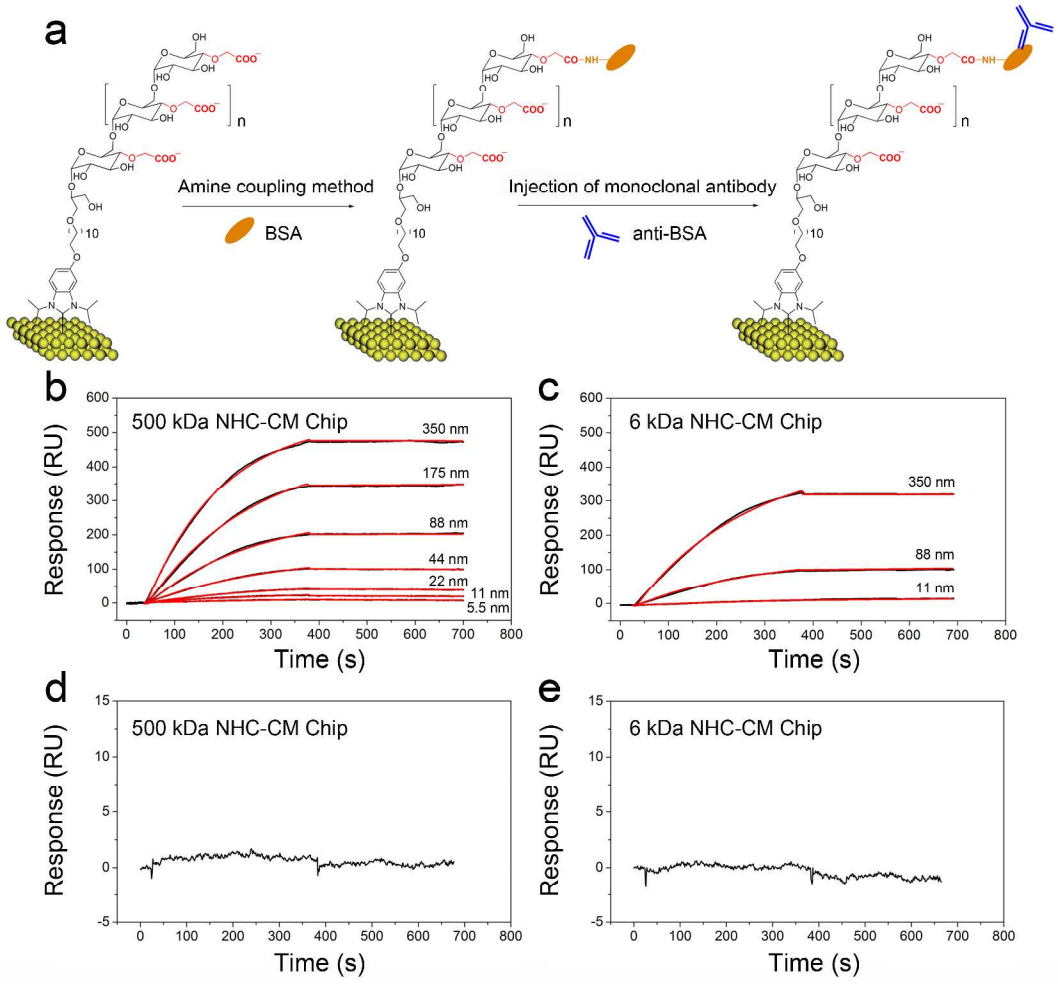

Figure 5. (a) BSA immobilized on dextran-modified NHC chip by amine coupling chemistry, followed by interaction with anti-BSA. Sensorgrams (black lines) and fitting curves (red lines) of anti-BSA binding to pre-immobilized BSA on (b) 500 kDa NHC-CM and (c) 6 kDa NHC-CM chips. Concentrations are noted as described in Section 2.5.2 of the experimental section. Biotin anti-mouse IgG2b antibody (50 nM) was used as a negative control to bind on BSA immobilized (d) 500 kDa NHC-CM and (e) 6 kDa NHC-CM chips.

Figures 5b and c show the sensorgrams and fitting curves for multiple concentrations of anti-BSA injected over pre-immobilized BSA on the 500 kDa NHC-CM and 6 kDa NHC-CM surfaces. At t = 0 s, buffer was flowed over the BSA immobilized sensor surface through a microfluidic system. At t = 40 s, a solution of anti-BSA was passed over the pre-immobilized BSA surface. As the antibody-antigen complex was formed on the sensor surface, the refractive index of the medium near the sensor surface changed accordingly, which can be monitored by the SPR detector. Thus, the association rate constant (k_a) of the interaction can be determined. At t = 400 s, the antibody solution was replaced by buffer, and the antibody-antigen complex was then allowed to dissociate, allowing the determination of the dissociation rate constant (k_d) for the interaction. The binding assays at varying concentrations of analyte gives a robust data set which may be fit using a 1:1 Langmuir binding model.[50,55–57]

Of note is that, from a technical perspective, these figures demonstrate the high quality of the binding results obtained on both NHC-based surfaces.[32,47] In each case, the response intensities are proportional to the injected anti-BSA concentrations. Moreover, the responses and the fitting curves superimposed over each data set, implying the reliability of the reported kinetics for the interactions.[4,32,47] Using the kinetic analysis of anti-BSA/BSA interaction on the 500 kDa NHC-CM chip (Table S7) yields a k_a of $(8.9 \pm 2.0) \times 10^4$ $M^{-1}s^{-1}$ and a k_d of $(1.2 \pm 0.2) \times 10^{-4}$ s^{-}

[1], affording an equilibrium dissociation constant (K_D) of (1.4 ± 0.5) × 10^{-9} M. A similar analysis on the 6 kDa NHC-CM chip (Table S7) yields values of k_a, k_d, and K_D of (1.1 ± 0.2) × 10^5 $M^{-1}s^{-1}$, (1.6 ± 0.3) × 10^{-4} s^{-1}, and (1.5 ± 0.5) × 10^{-9} M, respectively.

Although the magnitude of the binding response was observed to be greater for the 500 kDa NHC-CM chip as compared to the 6 kDa NHC-CM (which possesses a thinner dextran layer), the overall character of the binding curves and the corresponding binding parameters were observed to be similar. Specifically, the values of K_D obtained from the 500 kDa NHC-CM and 6 kDa NHC-CM chips are consistent with one another and lie within the expected K_D range of reported data in the literature, being 2.9 × 10^{-8} M and (1.7 ± 0.2) × 10^{-9} M for commercial thiol-based dextran-functionalized (CM5) chips,[55,56] and 3.6 × 10^{-9} M and 7.9 × 10^{-9} M for commercial thiol-based carboxyl-terminated SAM surfaces.[56,57] Additionally, a control experiment was performed using a biotin anti-mouse IgG2b antibody as an analyte, which contributes negligible signal (Figures 5d,e). This demonstrates that the observed binding curves (Figures 5b,c) were representative of the highly specific binding of anti-BSA to BSA, as well as low non-specific levels for both of these surfaces. While comparison to literature values is difficult, due to the fact that antibodies from different sources can display different reactivity and kinetics, the data from our comparative study implies that the binding constants measured by the NHC-based platform were equivalent to those determined by the commercial thiol-based platform. These results further validate the potential use of the NHC sensor surfaces for studies of high-affinity antibody-antigen interactions.

CONCLUSIONS

In this study, we have characterized potential biosensor surfaces supported by NHC SAMs as an alternative to thiol-supported biosensor surfaces. In addition to SPR performance validation

tests of NHC-supported dextran surfaces with drug-plasma protein and antibody-antigen interactions, we have evaluated non-specific binding resistance, thermal stability, and surface homogeneity of NHC-dextran surfaces versus thiol-based biosensor surfaces. In terms of the SPR performance, we found that the NHC-supported dextran surfaces yielded comparable performance to commercial thiol-supported biosensor surfaces when conducting kinetic analysis of two different model biomolecular kinetic interaction systems. Standardized SPR instrument tests also showed the NHC-dextran surfaces to be homogeneous and sufficiently responsive to enable the instrument to meet performance check standards. Our results show that, when properly designed and applied, the NHC-based platform has the potential that allows facile tuning of surface properties, enabling various ligands to be efficiently immobilized for subsequent biomolecular interactions. Assessments of the thermal stability of thiol-supported and NHC-supported biosensor surfaces by XPS, wettability, AFM as well as SPR tests for non-specific protein adsorption, showed that the NHC-supported surface possesses greater thermal resistance. The above performance and stability strengths of the NHC-supported dextran surfaces demonstrate its potential as alternative biosensing platform, and its versatility for modification confers promise for greater future applications in life science research.

ASSOCIATED CONTENT

Supporting Information.

Preparation procedure of dextran-modified thiol-based sensor surface, and an extended dataset of AFM images, XPS, contact angles, surface roughness, view dips, system check, non-specific protein adsorption, plasma protein-drugs, and antibody-antigen tests.

The Supporting Information is available free of charge on the ACS Publications website at DOI:

AUTHOR INFORMATION

Corresponding Author

E-mail: hongxiah@cupl.edu.cn

E-mail: jhh@queensu.ca; Phone: +44 (01323) 834467

Notes

The authors declare no competing financial interest.

ACKNOWLEDGMENT

H.H. and Z.L gratefully acknowledge the Humanities and Social Science Research program of China University of Politics and Law (10ZFQ82009), Academician Foundation of the Ministry of Public Security of the People's Republic of China (2011-23214203, 2011-23215243, 2011-23317015), Beijing Municipal Education Commission University Science and Technology Park Construction Project (2011-08111603), and Program for Young Innovative Research Team in China University of Political Science and Law (2014CXTD04,16CXTD05) for financial support. Z.L, M.R.N, C.M.C, and J.H.H acknowledge the Natural Sciences and Engineering Research Council of Canada (NSERC) for support in terms of discovery and CREATE grants. The Canada Foundation for Innovation (CFI) is acknowledged for infrastructure support.

REFERENCES

(1) Love, J. C.; Estroff, L. A.; Kriebel, J. K.; Nuzzo, R. G.; Whitesides, G. M. Self-Assembled Monolayers of Thiolates on Metals as a Form of Nanotechnology. *Chem. Rev.* **2005**, *105*, 1103−1169.

(2) Gooding, J. J.; Ciampi, S. The Molecular Level Modification of Surfaces: from Self-Assembled Monolayers to Complex Molecular Assemblies. *Chem. Soc. Rev.* **2011**, *40*, 2704–2718.

(3) Schasfoort, R. B. M.; Tudos, A. J. *Handbook of Surface Plasmon Resonance*; RSC Publishing, 2008.

(4) Cooper, M. A. *Label-Free Biosensors: Techniques and Applications*; Cambridge University Press, 2009.

(5) Gopinath, S. C. B. Biosensing Applications of Surface Plasmon Resonance-Based Biacore Technology. *Sensors and Actuators B* **2010**, *150*, 722–733.

(6) Masson, J.-F. Surface Plasmon Resonance Clinical Biosensors for Medical Diagnostics. *ACS Sens*. **2017**, *2*, 16−30.

(7) Labib, M.; Sargent, E. H.; Kelley, S. O. Electrochemical Methods for the Analysis of Clinically Relevant Biomolecules. *Chem. Rev*. **2016**, *116*, 9001−9090.

(8) Löfås, S.; Johnsson, B. A Novel Hydrogel Matrix on Gold Surfaces in Surface Plasmon Resonance Sensors for Fast and Efficient Covalent Immobilization of Ligands. *J. Chem. Soc. Chem. Commun.* **1990**, *21*, 1526–1528.

(9) Löfås, S. Dextran Modified Self-Assembled Monolayer Surfaces for Use in Biointeraction Analysis with Surface Plasmon Resonance. *Pure & Appl. Chem.* **1995**, *67*, 829–834.

(10) Granqvist, N.; Yliperttula, M.; Välimäli, S.; Pulkkinen, P.; Tenhu, H.; Viitala, T. Control of the Morphology of Lipid Layers by Substrate Surface Chemistry. *Langmuir* **2014**, *30*, 2799−2809.

(11) Schlenoff, J. B.; Li, M.; Ly, H. Stability and Self-Exchange in Alkanethiol Monolayers. *J. Am. Chem. Soc.* **1995**, *117*, 12528–12536.

(12) Vericat, C.; Vela, M. E.; Benitez, G.; Carro, P.; Salvarezza, R. C. Self-Assembled Monolayers of Thiols and Dithiols on Gold: New Challenges for a Well-Known System. *Chem. Soc. Rev.* **2010**, *39*, 1805–1834.

(13) Perrino, C.; Lee, S.; Choi, S. W.; Maruyama, A.; Spencer, N. D. A Biomimetic Alternative to Poly(ethylene glycol) as an Antifouling Coating: Resistance to Nonspecific Protein Adsorption of Poly(L-lysine)-*graft*-dextran. *Langmuir* **2008**, *24*, 8850–8856.

(14) Flynn, N. T.; Tran, T. N. T.; Cima, M. J.; Langer, R. Long-Term Stability of Self-Assembled Monolayers in Biological Media. *Langmuir* **2003**, *19*, 10909–10915.

(15) Romashov, L. V.; Ananikov, V. P. Self-Assembled Selenium Monolayers: From Nanotechnology to Materials Science and Adaptive Catalysis. *Chem. Eur. J.* **2013**, *19*, 17640 – 17660.

(16) Huang, F. K.; Horton, R. C.; Myles, D. C.; Garrell, R. L. Selenolates as Alternatives to Thiolates for Self-Assembled Monolayers: A SERS Study. *Langmuir* **1998**, *14*, 4802 − 4808.

(17) Hopkinson, M. N.; Richter, C.; Schedler, M.; Glorius, F. An Overview of N-Heterocyclic Carbenes. *Nature* **2014**, *510*, 485–496.

(18) Crudden, C. M.; Horton, J. H.; Ebralidze, I. I.; Zenkina, O. V.; McLean, A. B.; Drevniok, B.; She, Z.; Kraatz, H.-B.; Mosey, N. J.; Seki, T.; Keske, E. C.; Leake, J. D.; Rousina-Webb, A.; Wu, G. Ultra Stable Self-Assembled Monolayers of N-Heterocyclic Carbenes on Gold. *Nat. Chem.* **2014**, *6*, 409–414.

(19) Zhukhovitskiy, A. V.; MacLeod, M. J.; Johnson, J. A. Carbene Ligands in Surface Chemistry: From Stabilization of Discrete Elemental Allotropes to Modification of Nanoscale and Bulk Substrates. *Chem. Rev.* **2015**, *115*, 11503–11532.

(20) Wang, G.; Rühling, A.; Amirjalayer, S.; Knor, M.; Ernst, J. B.; Richter, C.; Gao, H.-J.; Timmer, A.; Gao, H.-Y.; Doltsinis, N. L.; Glorius, F.; Fuchs, H. Ballbot-Type Motion of N-Heterocyclic Carbenes on Gold Surfaces. *Nat. Chem.* **2016**, 152–156.

(21) Crudden, C. M.; Horton, J. H.; Narouz, M. R.; Li, Z.; Smith, C. A.; Munro, K.; Baddeley, C. J.; Larrea, C. R.; Drevniok, B.; Thanabalasingam, B.; McLean, A. B.; Zenkina, O. V.; Ebralidze, I. I.; She, Z.; Kraatz, H.-B.; Mosey, N. J.; Saunders, L. N.; Yagi, A. Simple Direct Formation of Self-Assembled N-Heterocyclic Carbene Monolayers on Gold and Their Application in Biosensing. *Nat. Commun.* **2016**, *7*, 12654–12660.

(22) Solomatina, A. I.; Chelushkin, P. S.; Krupenya, D. V.; Podkorytov, I. S.; Artamonova, T. O.; Sizov, V. V.; Melnikov, A. S.; Gurzhiy, V. V.; Koshel, E. I.; Shcheslavskiy, V. I.; Tunik, S. P. Coordination to Imidazole Ring Switches on Phosphorescence of Platinum Cyclometalated Complexes: The Route to Selective Labeling of Peptides and Proteins via Histidine Residues. *Bioconjugate Chem.* **2017**, *28*, 426−437.

(23) Wang, D.; Jong, D. H. de.; Rühling, A.; Lesch, V.; Shimizu, K.; Wulff, S.; Heuer, A.; Glorius, F.; Galla, H.-J. Imidazolium-Based Lipid Analogues and Their Interaction with Phosphatidylcholine Membranes. *Langmuir* **2016**, *32*, 12579−12592.

(24) Wang, D.; Richter, C.; Rhling, A.; Drcker, P.; Siegmund, D.; Metzler-Nolte, N.; Glorius, F.; Galla, H.-J. A Remarkably Simple Class of Imidazolium-Based Lipids and Their Biological Properties. *Chem. Eur. J.* **2015**, *21*, 15123–15126.

(25) Ratel, M.; Provencher-Girard, A.; Zhao, S. S.; Breault-Turcot, J.; Labrecque-Carbonneau, J.; Branca, M.; Pelletier, J. N.; Schmitzer, A. R.; Masson, J.-F. Imidazolium-Based Ionic Liquid Surfaces for Biosensing. *Anal. Chem.* **2013**, *85*, 5770–5777.

(26) Salorinne, K.; Man, R. W. Y.; Li, C-H.; Taki, M.; Nambo, M.; Crudden, C. M. Water Soluble N-Heterocyclic Carbene-Protected Gold Nanoparticles: Synthesis, Stability and Optical Properties. *Angewandte Chem. Intl. Ed.* **2017**, *56*, 6198-6202.

(27) Gopinath, S. C. B. Biosensing Applications of Surface Plasmon Resonance-Based Biacore Technology. *Sensors and Actuators B* **2010**, *150*, 722–733.

(28) Mauriz, E.; García-Fernández, M. C.; Lechug, L. M. Towards the Design of Universal Immunosurfaces for SPR-Based Assays: A Review. *Trends Anal. Chem.* **2016**, *79*, 191–198.

(29) Van der Merwe, P. A. *Surface Plasmon Resonance. In Protein-Ligand Interactions: Hydrodynamics and Calorimetry*; Oxford University Press, 2001.

(30*) BIACORE ® 3000 Instrument Handbook*; Biacore AB, 1999.

(31) Frostell-Karlsson, Å.; Remaeus, A.; Roos, H.; Andersson, K.; Borg, P.; Hämäläinen, M.; Karlsson, R. Biosensor Analysis of the Interaction Between Immobilized Human Serum Albumin and Drug Compounds for Prediction of Human Serum Albumin Binding Levels. *J. Med. Chem.* **2000**, *43*, 1986–1992.

(32) Myszka, D. G. Improving Biosensor Analysis. *J. Mol. Recognit.* **1999**, *12*, 279–284.

(33) Rich, R. L.; Day, Y. S. N.; Morton, T. A.; Myszka, D. G. High-Resolution and High-Throughput Protocols for Measuring Drug/Human Serum Albumin Interactions Using BIACORE. *Anal. Biochem.* **2001**, *296*, 197–207.

(34) Characterization of Drug-Plasma Protein Interactions Using Surface Plasmon Resonance. Biacore Application Note 30.

(35) Saftics, A.; Kurunczi, S.; Szekrényes, Z.; Kamarás, K.; Khánh, N. Q.; Sulyok, A.; Bősze, S.; Horvath, R. Fabrication and Characterization of Ultrathin Dextran Layers: Time Dependent

Nanostructure in Aqueous Environments Revealed by OWLS. *Colloids Surf. B* **2016**, *146*, 861–870.

(36) Vlugt-Wensink, K. D. F.; Jiang, X.; Schotman, G.; Kruijtzer, G.; Vredenberg, A.; Chung, J. T.; Zhang, Z.; Versluis, Cees.; Ramos, D.; Verrijk, R.; Jiskoot, W.; Crommelin, D. J. A.; Hennink, W. E. In Vitro Degradation Behavior of Microspheres Based on Cross-Linked Dextran. *Biomacromolecules* **2006**, *7*, 2983–2990.

(37) Dai, F.; Du, M.; Liu, Y.; Liu, G.; Liu, Q.; Zhang, X. Folic Acid-Conjugated Glucose and Dextran Coated Iron Oxide Nanoparticles as MRI Contrast Agents for Diagnosis and Treatment Response of Rheumatoid Arthritis. *J. Mater. Chem. B* **2014**, *2*, 2240–2247.

(38) Pleteníková, M.; Matisová-Rychlá, L.; Rychlý, J.; Lacík, I. Chemiluminescence Related to Degradation of Thermally Oxidized Pullulans. Comparison with Cellulose and Dextran. *Carbohydr. Polym.* **2007**, *69*, 50–64.

(39) Duwez, A. S. Exploiting Electron Spectroscopies to Probe the Structure and Organization of Self-Assembled Monolayers: A Review. *J. Electron. Spectrosc. Relat. Phenom.* **2004**, *134*, 97–138.

(40) Laibinis, P. E.; Whitesides, G. M.; Allara, D. L.; Tao, V. T.; Parikh, A. N.; Nuzzo, R. G. Comparison of the Structures and Wetting Properties of Self-Assembled Monolayers of n-Alkanethiols on the Coinage Metal Surfaces, Cu, Ag, Au. *J. Am. Chem. Soc.* **1991**, *113*, 7152–7167.

(41) Love, J. C.; Wolfe, D. B.; Haasch, R.; Chabinyc, M. L.; Paul, K. E.; Whitesides, G. M.; Nuzzo, R. G. Formation and Structure of Self-Assembled Monolayers of Alkanethiolates on Palladium. *J. Am. Chem. Soc.* **2003**, *125*, 2597–2609.

(42) Zhukhovitskiy, A. V.; Mavros, M. G.; Voorhis, T. V.; Johnson, J. A. Addressable Carbene Anchors for Gold Surfaces. *J. Am. Chem. Soc.* **2013**, *135*, 7418–7421.

(43) Roland, S.; Ling, X.; Pileni, M.-P. N-Heterocyclic Carbene Ligands for Au Nanocrystal Stabilization and Three-Dimensional Self-Assembly. *Langmuir* **2016**, *32*, 7683–7696.

(44) Tasker, S.; Matthijs, G.; Davies, M. C.; Roberts, C. J.; Schacht, E. H.; Tendler, S. J. B. Molecular Resolution Imaging of Dextran Monolayers Immobilized on Silica by Atomic Force Microscopy. *Langmuir* **1996**, *12*, 6436–6442.

(45) Frazier, R. A.; Matthijs, G.; Davies, M. C.; Roberts, C. J.; Schacht, E.; Tendler, S. J. B. Characterization of Protein-Resistant Dextran Monolayers. *Biomaterials* **2000**, *21*, 957–966.

(46) Touzov, I.; Gorman, C. B. Tip-Induced Structural Rearrangements of Alkanethiolate Self-Assembled Monolayers on Gold. *J. Phys. Chem. B* **1997**, *101*, 5263–5276.

(47) Marquart, J. A. *Surface Plasma Resonance and Biomolecular Interaction Analysis: Theory and Practice*; Nederland, 2014.

(48) Jeon, S. I.; Lee, J. H.; Andrade, J. D.; Gennes, P. G. De. Protein-Surface Interactions in the Presence of Polyethylene Oxide: I. Simplified Theory, *J. Colloid Interface Sci*. **1991**, *142*, 149–158.

(49) Malmström, J.; Nieuwoudt, M. K.; Strover, L. T.; Hackett, A.; Laita, O.; Brimble, M. A.; Williams, D.; Travas-Sejdic, J. Grafting from Poly(3,4-ethylenedioxythiophene): A Simple Route to Versatile Electrically Addressable Surfaces. *Macromolecules* **2013**, *46*, 4955−4965.

(50) *BIAevaluation 3.0 Software Handbook*; Biacore AB, 1997.

(51) APPLICATION NOTE: 121 BioNavis.

(52) Chen, X.; Zhou, G.; Song, P.; Wang, J.; Gao, J.; Lu, J.; Fan, C.; Zuo, X. Ultrasensitive Electrochemical Detection of Prostate-Specific Antigen by Using Antibodies Anchored on a DNA Nanostructural Scaffold. *Anal. Chem.* **2014**, *86*, 7337−7342.

(53) Dinh, T. L.; Ngan, K. C.; Shoemaker, C. B.; Walt, D. R. Using Antigen-Antibody Binding Kinetic Parameters to Understand Single-Molecule Array Immunoassay Performance. *Anal. Chem.* **2016**, *88*, 11335–11339.

(54) Farka, Z.; Juřík, T.; Pastucha, M.; Skládal, P. Precipitation Enhanced Surface Plasmon Resonance Immunosensor for the Detection of Salmonella in Powdered Milk. *Anal. Chem.* **2016**, *88*, 11830–11836.

(55) Liu, Y.; Lin, M.; Zhang, X.; Hu, X.; Lin, J.; Hao, J.; He, D.; Zhang, X.; Xu, C.; Zhong, J.; Xie, Y.; Zhang, C.; Liu, X. Development of Competitive ELISA for the Detection of Bovine Serum Albumin using Single-Chain Variable Fragments. *Anal. Biochem.* **2017**, *525*, 89–91.

(56) APPLICATION NOTE: 107 Biosensing Instrument.

(57) http://www.colby.edu/chemistry/PChem/lab/SPRBSAAntiBSA.pdf

Table of Contents